Al-Khwarizmi Engineering Journal
ISSN (printed): 1818 – 1171, ISSN (online): 2312 – 0789
Vol. 20, No. 4, December (2024), pp. 25-37

Al-Khwarizmi Engineering Journal

CuO/ZnO Nanocomposite Biosynthesis Approach Using Eucalyptus Leaves for Photodegradation of Tetracycline

Marwa S. Ameer[1], Mohammed A. Atiya[2]*, Ahmed K. Hassan[3], Abdelmalik Milad Shakorfow[4], Najah Al Mhanna[5]

[1,2]*Department of Biochemical Engineering, Al-khwarizmi College of Engineering, University of Baghdad, Baghdad, Iraq*
[3]*Environment, Water, and Renewable Energy Directorate, Ministry of Science and Technology, Baghdad, Iraq*
[4]*Elmergib University, Libya*
[5]*German University of Technology in Oman, Oman*
*Corresponding Author's E-mail: atiya@kecbu.uobaghdad.edu.iq

(Received 24 May 2024; Revised 5 July 2024; Accepted 11 August 2024; Published 1 December 2024)
https://doi.org/10.22153/kej.2024.08.003

Abstract

In this study, the photocatalytic degradation of tetracycline (TC), which is responsible for water pollution, was investigated in an aqueous solution by using two types of nanoparticles (NPs) based on green synthesis of ZnO NPs and CuO NPs as photocatalysts. Eucalyptus plant extract was chosen as a good reductant and capping agent because of its cost-effectiveness, nontoxic characteristics and ease of usage. Different molar ratios of Cu:Zn (1:3, 1:6, 1:9 and 1:12) were prepared, and then these ratios were evaluated to select the effective ratio for removing TC. The 1:6 ratio demonstrated the best photocatalytic performance, degrading 72.15% of TC at the ZnO/CuO nanocomposite (NC) dose of 0.5 g/L, an initial concentration of 10 mg/L, pH 7, an agitation speed of 300 rpm, a temperature of 25 °C, UV intensities of 15 W/m^2 and a contact time of 180 min. The synthesis of NCs was characterised using different analysis methods. CuO/ZnO characteristics were investigated using several analytical techniques, including FTIR, FESEM, EDAX, AFM, BET and zeta potential analysis. The NP's structure, morphology, thermal behaviour, chemical composition and optical properties were analysed. The FESEM images verified that the (1:6) CuO/ZnO NPs calcined and not calcined, with sizes of 13.92 and 26.73 nm, respectively, were crystalline and spherical. The quantity of TC degradation by metal oxide NCs was investigated using UV–Vis spectroscopy. This method is sustainable and environmentally benign because it synthesises both NPs from plant sources. These hybrid nanoparticles may be used to treat other pharmaceuticals that are hazardous to reduce pollution in water.

Keywords: *CuO/ZnO nanoparticles; Eucalyptus; Green synthesis; Photocatalyst process; Tetracycline (TC)*

1. Introduction

Human and veterinary medications are one of the leading sources of contamination in natural water systems owing to their widespread usage nowadays. Many antibiotics are released into rivers together with medical waste and wastewater from pharmaceutical plants. Antibiotics in aquatic environments are a substantial source of environmental contamination [1]. Conventional water and wastewater treatment plants cannot entirely remove antibiotics and other pharmaceutical compounds. As a result, antibiotics are released into the environment through wastewater, exposing humans, aquatic species and plants to them. For these reasons, future research must focus on developing suitable treatment systems that may be integrated into water and wastewater facilities [2].

Tetracycline (TC) antibiotics are the second most commonly employed antibiotics globally, producing and using antibiotics widely utilised today to treat various infectious disorders. This antibiotic's presence in the environment harms human health and ecological function [3]. In 2002, the worldwide usage of antibiotics was between

100,000 and 200,000 tons per year. By 2015, this amount had risen to 34.8 billion, representing a significant increase of 65% since 2000. It is projected that by 2020, the consumption of antibiotics will reach 4.5 trillion doses [4]. Hospitals, pharmaceutical industries, and livestock contribute to the buildup of TC in wastewater systems [5]. Domestic wastewater has a low content of TCs, namely, 1 mg L^{-1}, whereas hospital wastewater has a considerably larger concentration of TCs, specifically 100 mg L^{-1} [6, 7]. Thus, an effective technique to eliminate harmful compounds is necessary [3]. Various methods were used to remove pollutants, such as physical [8], chemical and biological procedures like adsorption [9], membrane process [10], chemical oxidation [11], ozonation [12], ultrasound [13] and membrane reactors to eliminate antibiotic residues, including TC [14]. Advanced oxidation processes (AOPs) are effective methods of degrading harmful and biodegradable contaminants in aquatic environments [3], as shown in Figure 1. AOPs, including photolysis, ozonation, Fenton and photo-Fenton processes and the oxidation of antibiotics in the presence of ozone/UV/hydrogen peroxide, primarily include the transformation and release of oxidised products.

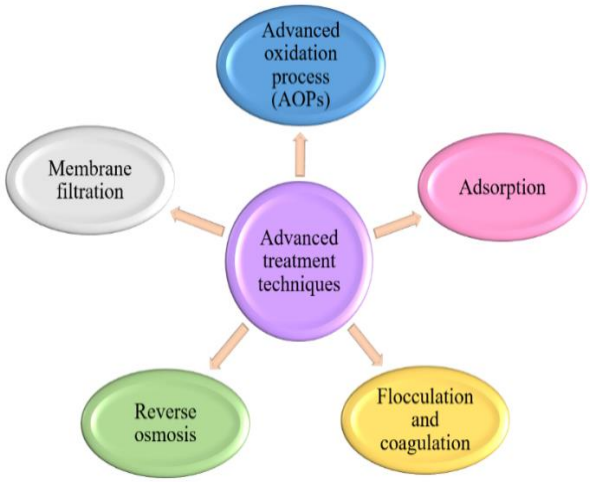

Fig. 1 Advanced processes for the removal of TC.

Nanotechnologies have recently become important in eradicating environmental contaminants. Nano-adsorbents exhibit better adsorption capacity than traditional adsorbents due to their larger specific surface area and enhanced selectivity. This is achieved through precise surface modification of the nanomaterial to target impurities in particular [15]. By utilising plant extracts or bio-organisms, green synthesis is a simple substitute for chemical synthesis. It offers several advantages over chemical processes, including scaling up systems whilst ensuring economic viability, environmental friendliness and operational efficiency [16]. Photocatalytic remediation for removing antibiotic contaminants from water is an extremely promising method. The process can potentially convert organic contaminants in effluent into innocuous molecules whilst being environmentally sustainable [17]. Photodegradation, when combined with the application of chemical compounds like TiO_2 and ZnO suspensions, is a very promising technology for rapidly degrading TC. This method has been extensively studied and shown to be effective in previous research [13, 23, 24]. The advantageous properties and wide-ranging uses of metal oxide nanoparticles (NPs) have garnered significant interest across various disciplines in recent decades. ZnO and CuO are two examples of NPs [20]. ZnO and CuO NPs are widely used because they have unique chemical, physical and mechanical properties, including low melting point, large surface area, excellent structural stability, rapid diffusion and high surface energy [21]. ZnO is classified as an n-type semiconductor because of its notable direct energy band gap measuring 3.37 eV. Meanwhile, CuO is categorised as a p-type semiconductor owing to its comparatively narrower band gap of 2.5 eV. The incorporation of ZnO NPs into the CuO matrix was effectively carried out through environmentally sustainable synthesis methods, leading to a band gap reduction of 1.45 electron volts relative to the initial constituents [22].

CuO/ZnO NCs were formed using biological systems, particularly extracts obtained from diverse plant constituents (including leaves, seeds, pith and bark) and biomass generated from bacteria, algae and fungi. Innovative precursor substances were produced in the structure of biogenic molecules [23]. Recent proposals suggest that for the synthesis of CuO/ZnO NCs, leaf extracts are a superior alternative to currently available biological systems. This technology promotes environmental sustainability and reduces costs by eliminating the requirements for biological material collection, storage, manipulation and disposal [24]. Various techniques are employed to characterise the composites, including energy dispersive X-ray spectroscopy (EDAX), Fourier transform infrared (FTIR) spectroscopy, atomic force microscopy (AFM), Brunauer–Emmett–Teller (BET) method, zeta potential (ZP) and field-emission scanning electron microscopy (FESEM). Eucalyptus serves as a reliable source of bioactive compounds. The ecological methodology produces NPs by utilising terpenoids, phenols and their derivatives. Moreover,

this plant is easily accessible in most nations [15]. The well-known perennial tree *Eucalyptus globulus* is utilised in numerous industries, including construction, biology, medicine, flavouring, fragrance and essential oil production [25]. In the present study, CuO/ZnO NCs were produced by blending the two components in different ratios by utilising an extract obtained from the foliage of the eucalyptus plant. These ratios were evaluated to determine the best ratio for eliminating TC from water.

2. Experimental Procedures

2.1. Chemicals and Reagents

The target adsorbate TC was provided by The State Enterprise for Drug Industries and Medical Appliances in Samara, Iraq, Table 1 outlines TC's primary characteristics. The eucalyptus leaves used were picked up from a yard at the University of Baghdad, Iraq. $ZnSO_4.7H_2O$ with a purity of > 98.0% and $CuSO_4{\cdot}5H_2O$ with a purity of > 99% were purchased from CDH company, India, and Alpha Chemicals, India, respectively. NaOH was acquired from CDH Company. Absolute ethanol was purchased from Carlo Erba's company.

Table 1.
Properties of tetracycline

Name of antibiotic	Tetracycline
Molecular formula	$C_{22}H_{24}N_2O_8$
Chemical structure	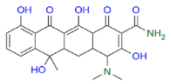
Molecular weight (MW)	480.9 g
Colour	Yellow
Solubility	Light

2.2. Leaf extract preparation

CuO/ZnO nanocrystals were manufactured using the same process as described in a previous research [26], with some modifications. The leaves of the eucalyptus plant were collected from the grounds of University of Baghdad. They were cleaned many times with distilled water and then dried for 12 h at 50 °C in an oven. Once completely dried and able to be crushed, the leaves were ground into a powder and sieved using a 63 µm sieve. Subsequently, 15 g of eucalyptus leaf powder was introduced into 200 mL of deionised water and heated with magnetic stirring for 30 min at 85 °C ± 5 °C, as shown in Figure 2. The resultant extract was chilled and subsequently allowed to reach room temperature. It was then filtered using vacuum filtration using Whitman filter paper number 2 to remove suspended leaves. The resulting solution was enclosed in a glass bottle and stored in a refrigerator at 4 °C for use in the next experiments.

Fig. 2. Diagram of eucalyptus extract preparation

2.3. Synthesis of CuO/ZnO Nanocomposites (NCs)

Green synthesis of ZnO/CuO NCs was conducted by altering the prescribed ratios for this experiment. Table 2 lists the mass of $CuSO_4{\cdot}5H_2O$ and $ZnSO_4.7H_2O$ in the molar ratios of Cu/Zn as (1:3), (1:6), (1:9) and (1:12).

Table 2.
Weight parameters of copper sulphate and zinc sulphate salts in synthesising CuO/ZnO heterojunctions.

Salt	Molar ratio of Cu/Zn			
	1:3	**1:6**	**1:9**	**1:12**
$CuSO_4.5H_2O$	0.6884	0.3888	0.2709	0.2078
$ZnSO_4.7H_2O$	2.3116	2.6112	2.7291	2.7922

In accordance with Basit et al. [27], with minimal adjustments by utilising a chosen ratio, solid $ZnSO_4$ and $CuSO_4$ salts were added separately to 100 mL of deionised water and magnetically agitated at 150 rpm for 10 min, respectively. Once the salts were fully dissolved, the contaminants were eliminated by employing a 0.45 µm membrane filter. Subsequently, a solution of $ZnSO_4$ and $CuSO_4$ was combined for 15 min at 70 °C with continuous stirring. The eucalyptus extract was incrementally introduced into the zinc/copper salt solution, and the resulting combination was agitated at 70 °C. The solution's pH was modified to 10 by gradually adding a solution of NaOH (1 M). As a result, the solution's colour changed from dark brown to dark yellow, indicating the formation of CuO/ZnO NCs during the reduction process. The resultant mixture was continuously agitated and heated at 70 °C for 3 h.

After the reaction, the precipitate of NCs was obtained using vacuum filtering and promptly subjected to five washes with distilled water and three washes with ethanol to eliminate all contaminants and the remaining salt from the items. The precipitates were dehydrated in an oven at 60 °C for 10 h and transformed into a fine powder by using a mortar and pestle. The calcination process was carried out at 500 °C for a duration of 3 h by using a muffle furnace. Afterwards, the substance was left to passively cool to ambient temperature.

2.4. Characterisation of (CuO-ZnO) NCs

Various techniques were utilised to determine the surface area, structure, dimensions, size and chemical composition of CuO/ZnO NCs. The crystalline structure and degree of phase purity of the CuO/ZnO (NCs) synthesised via XRD were determined using a Phillips X'pert diffractometer. The "TESCAN-Vega3 model" was employed to acquire SEM images of the NPs, which were subsequently analysed to ascertain their structure, particle size and shape. An energy-dispersive X-ray spectroscopy EDAX analysis was conducted to determine the chemical compositions. The surface area of CuO/ZnO NCs was determined via BET test using a device model (TriStar II Plus Version 2.03, USA). FTIR analysis (Shimadzu, Japan) was employed to identify the functional groups present during the process. Zeta potential analysis was utilised to evaluate the NPs' stability. AFM (TT-2, USA) was utilised to determine the morphology and surface texture of CuO/ZnO NCs.

2.5. Analytical Method

A calibration curve was constructed for the standard antibiotic tetracaine TC solution before commencing the experiments to determine the maximum wavelength (λ_{max}) and establish the equation relating absorbance to concentration. According to Figure 3, the λ_{max} of TC was seen at 276 and 357 nm. The wavelength 357 nm is the most significant one for TC because it yields the highest absorbance [2]. The calibration plot of TC at the maximum wavelength of this antibiotic is shown in Figure 5. The percentage degradation efficiency (DE %) was estimated using the following formula, where C_o and C_t are the concentrations of TC at zero and time t, respectively, (mg. L^{-1}) [26]:

$$DE\% = \frac{Co - Ct}{Co} \times 100 \quad \ldots(1)$$

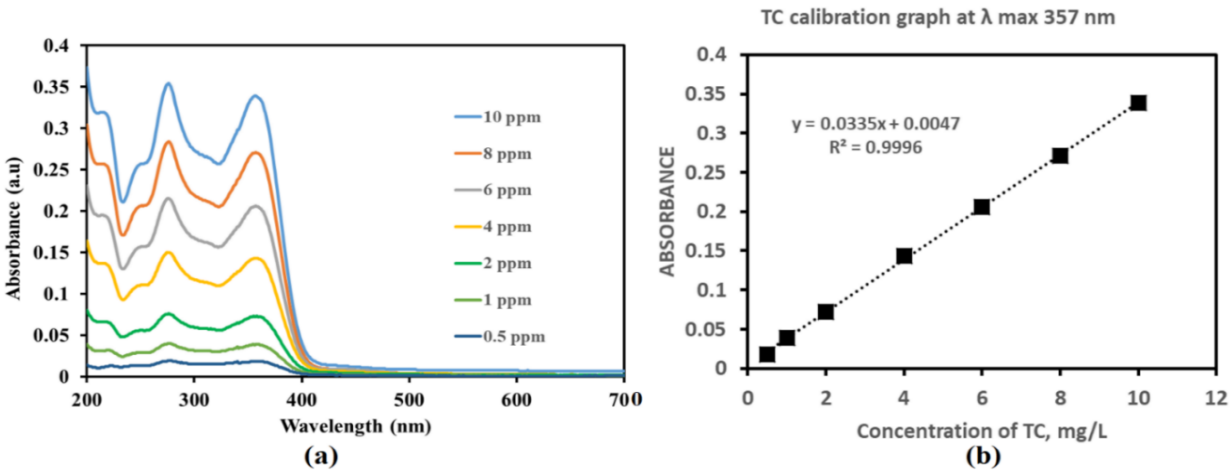

Fig. 3. (a) UV–Vis analysis for various concentrations of TC solutions. (b) Calibration plot at λ_{max} 357 nm.

2.6. Photocatalytic Activity

The effectiveness of ZnO/CuO NCs in photocatalysis was assessed by measuring the photodegradation of TC under different molar ratios of Cu to Zn (1:3, 1:6, 1:9 and 1:12), as shown in Table 1. This analysis aimed to identify the optimal molar ratio of Cu/Zn. The experimental parameters for the removal of TC for each ratio were used, with the catalyst doses of ZnO/CuO NCs at 0.5 g and a pH of 7. To achieve this, 1000 mL of a 10 ppm TC solution was mixed with the catalyst dose amounts in a 1 L beaker and continuously stirred at 300 rpm at room temperature. The mixture was left in the dark for 30 min to ensure adsorption–desorption equilibrium [28, 29]. Photocatalysis experiments were conducted utilising a semi-piolet-scale photoreactor that has been designed and is powered by 24 UV-A lamps with the following dimensions: 30 cm in length, 2.2 cm in width and a maximal wavelength peak of 365 nm. Afterwards, the experiments were conducted for 180 min; the λmax of TC chosen from the calibration curve was 357 nm. Throughout the assays, 10 mL of the specimens was collected at consistent time intervals (0, 5, 10, 15, 20, 25, 30, 45, 60, 90, 120 and 180 min) and filtered through a 0.45 m filter. The concentration of TC was measured using a Shimadzu-Japan UV-Vis spectrophotometer. The elimination rate was computed by employing Equation 1.

3. Results and Discussion

3.1 FE-SEM and EDAX Analyses

Figures 4 (a) and (b) show the FESEM images of calcined CuO/ZnO NCs and non-calcined NCs. The X-rays in SEM can be used to identify a sample's elemental composition by using EDAX.

The SEM images showed that the CuO/ZnO NCs have a semi-spherical morphology, with some degree of aggregation attributed to the presence of biomolecules from eucalyptus leaf extract that cap these NCs [30]. In Figure 4 (a), the synthesised NCs exhibited porous and spherical morphology, with an average diameter of ~14 nm. The SEM image indicates a randomly distributed sphere and few nanorods with an average diameter of ~27 nm, as shown in Figure 4 (b).

Figure 5 (a) and (b) show the EDAX spectrum, atomic distribution and elemental mapping topology of CuO/ZnO NCs with a molar ratio of Cu to Zn of 1:6, and the samples were calcined and not calcined. The intense peaks of Zn, Cu and O in the calcined CuO/ZnO NCs indicated the place of atomic distribution on the surface and the chemical composition. The weight percentages of Zn, Cu and O were 57.78 wt%, 0.20 wt%, and 42.02 wt%, respectively. By contrast, the intense peaks in the CuO/ZnO NCs without calcination showed weight percentages of 90.68 wt% for Zn, 0.10 wt% for Cu and 9.22 wt% for O. Small particles exhibit a large surface area due to their high surface-to-volume ratio. Consequently, a higher quantity of atoms was present on the surface of the particle than the atoms located on the inside. Surface atoms possess unoccupied valence or dangling bonds, rendering them highly reactive for the adsorption of other species or interaction with surrounding surface atoms, leading to the formation of particle clusters [31].

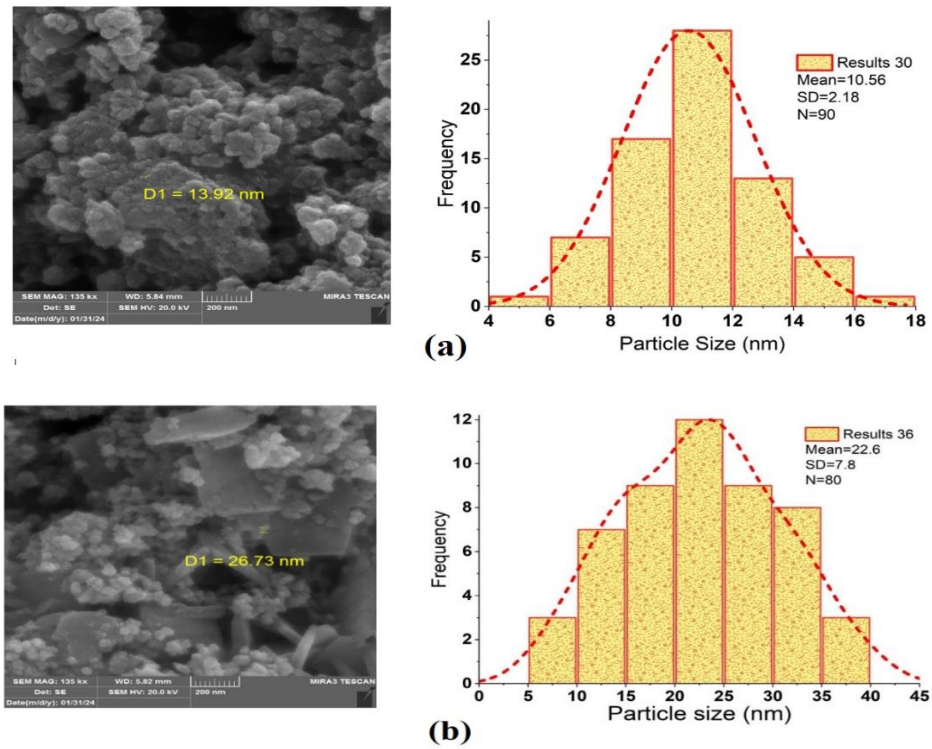

Fig. 4. SEM image of CuO/ZnO NCs: (a) calcined and (b) not calcined

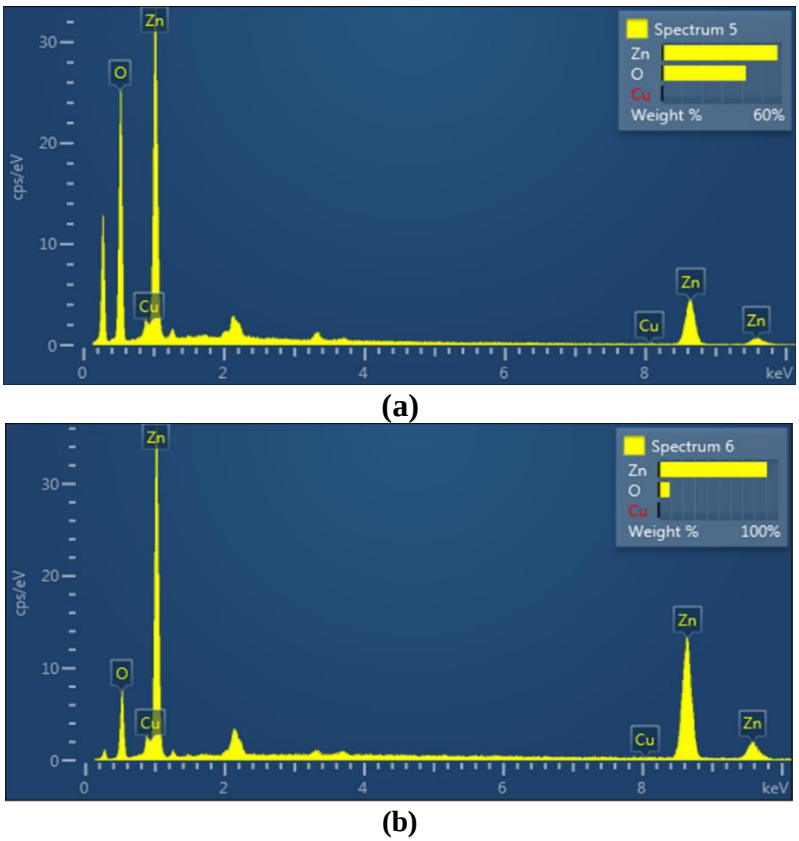

Fig. 5. EDAX analysis of CuO/ZnO NCs: (a) calcined and (b) not calcined

3.2 AFM

The size and morphology of CuO/ZnO NCs were assessed using AFM, which measures the force of contact between the tip and the surface. Figure 6 presents a three-dimensional representation of an AFM image, showcasing a uniform and smooth surface of NPs exhibiting

diverse sizes and compositions. The surface roughness of the NPs improves their capacity to absorb ions of organic pollutants [32]. The synthesised NPs were round and triangular. The average sizes were 76.95 nm for the calcined CuO/ZnO NCs with a molar ratio of 1:6 and 88.61 nm for the NCs without calcination according to AFM Figures 6 (a) and (b).

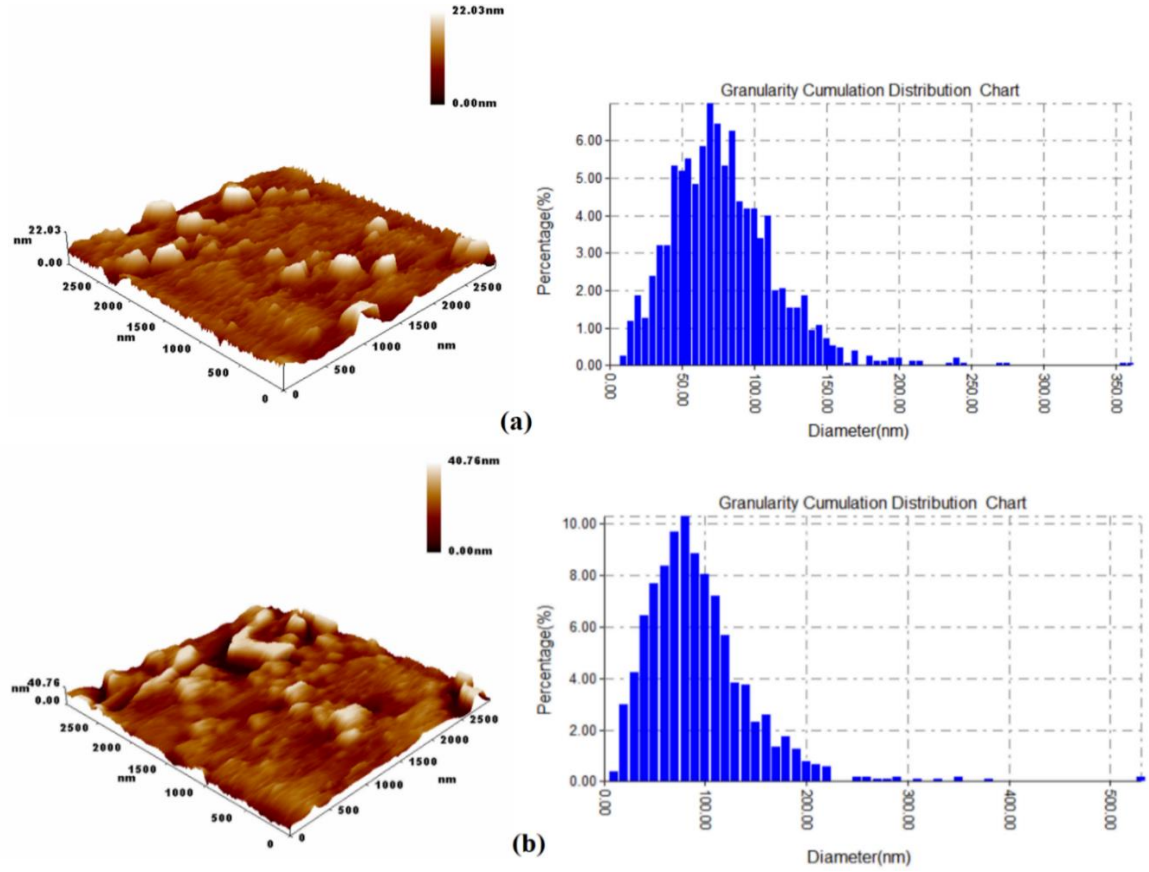

Fig. 6. Atomic force microscopic (AFM) characterisation for CuO/ZnO NCs: (a) calcined and (b) not calcined.

3.3 FTIR spectroscopy

FTIR spectroscopy (Shimadzu, Japan) was applied to determine the state of the catalysts and provide details on their functional groups and chemical bonds for all the four molar ratios of calcined CuO/ZnO NCs. The analysis used a mid-infrared spectrum ranging from 400 cm^{-1} to 4000 cm^{-1}, as shown in Figure 7. The peaks seen at 3618 and 3406 cm^{-1} are a result of the O–H stretching vibration, indicating the presence of polyphenol groups and supporting the existence of different capping and reduced bioactive molecules in the eucalyptus extract [30]. Phenolic compounds may be the cause of the stabilising process of NPs. The existence of a narrow absorption band indicates the occurrence of aromatic C−C stretching within the range of 865–870 cm^{-1}. The stretching modes of C–O seen at 1057 and 1188 cm^{-1} are present in the spectra of ZnO/CuO NCs and ascribed to the presence of adsorbed C=O on the surface of ZnO/CuO NCs due to the incomplete breakdown of the acetate group [25]. The presence of CuO/ZnO NCs was demonstrated by the 413 and 517 cm^{-1} peaks for all the four molar ratios of calcined CuO/ZnO NCs.

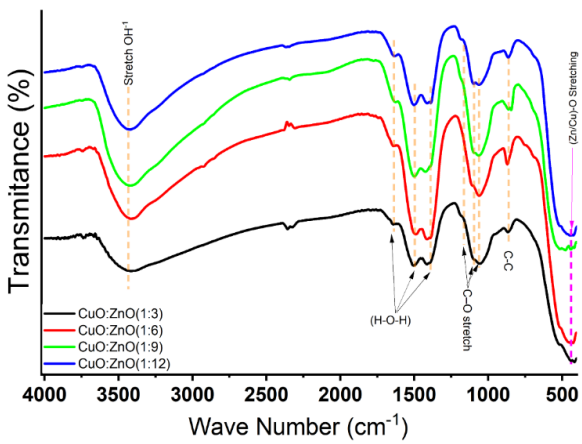

Fig. 7. Fourier transform infrared (FTIR) spectra of CuO/ZnO NCs with different molar ratios of Cu: Zn from 1:3 to 1:12

3.4 Powder XRD

XRD was used to characterise the crystalline structure and degree of phase purity of the synthesised CuO/ZnO NCs. The compositional analyses or phase identification for all samples were performed using Xpert-Pro software. The peaks in the XRD of the molar ratio of Cu:Zn at 1:3, 1:6, 1:9 and 1:12 were searched and then matched with the standard diffractograms given in the Joint Committee for Powder Diffraction Standards (JCPDS) database. The XRD patterns in Figure 8 showed that all the samples exhibited almost identical major diffraction peaks, suggesting that the crystal structures of the four samples, namely 1:3, 1:6, 1:9 and 1:12, were identical [29]. The former represents the standard XRD of hexagonally crystalline ZnO, whereas the latter represents monoclinic CuO.

The diffraction peaks for each of the molar ratios of Cu:Zn from 1:3 to 1:12 were located at (100), (002), (101), (102), (110), (103), (200), (112), (20 1), (004) and (202), with its corresponding 2θ values of ≈ 31.83°, 34.49°, 36.32°, 47.60°, 56.67°, 66.38°, 67.60°, 69.10°, 72.56° and 76.96°, respectively. These findings were in good agreement with the JCPDS of 00-036-1451 [28]. Typical peaks appeared with the diffraction peaks of the CuO sample acquired at the 2θ values of 32.51, 38.71, 46.26, 61,53, 74.98 and 79.73, which are due to (110), (111), (¯112), (¯113), (004) and (023), respectively. These data were found to be the same as those reported in Plans JCPDS of 00-048-1548. The increase in the molar ratio of Cu:Zn from 1:3 to 1:12 resulted in a drop in Cu content, which, in turn, reduced the strength of the distinctive diffraction peaks of CuO [33]. The product possesses a well-crystalline particle structure, as seen by the diffraction peaks that are narrow and robust [21].

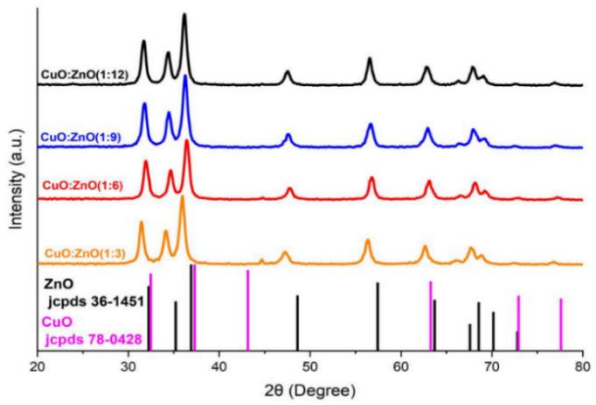

Fig. 8. XRD patterns of CuO/ZnO NCs with different molar ratios of Cu:Zn from 1:3 to 1:12

3.5 BET

Table (3) describes the surface area results of CuO/ZnO NCs obtained by the BET technique. The pore sizes of calcined and uncalcined CuO/ZnO NCs were 12.92151 and 11.63821 nm, respectively. According to the International Union of Pure and Applied Chemistry (IUPAC), a pore size in the 2–50 nm range indicates mesoporous, which enhances the catalytic activities due to the enhancement of the diffusion of materials [34].

Table 3.
BET parameters for CuO/ZnO NPs: (a) calcined and (b) not calcined
(a)

Parameter	Value
BET (m^2/g)	25.9477
Pore size (nm)	12.92151
Pore volume (cm^3/g)	0.083821

(b)

Parameter	Value
BET (m^2/g)	49.7492
Pore size (nm)	11.63821
Pore volume (cm^3/g)	0.144748

3.6 ZP Analysis

Measuring zeta potential is an essential method for ensuring the stability of particles. NPs demonstrate stability because of their increased zeta potential. A significant negative value proves the repulsion between particles, preventing the agglomeration of NCs and verifying their stability. Conversely, their diminished potential encourages and promotes flocculation. As shown in Figures 9 (a) and (b), the high negative values at −37.61and −29.01 mV acquired by zeta potential analysis revealed that excellent stability of CuO/ZnO NCs with and without calcination, respectively. The catalyst's stability is attributed to the application of a polyphenol coating derived from eucalyptus leaves onto the surface of the NCs [35].

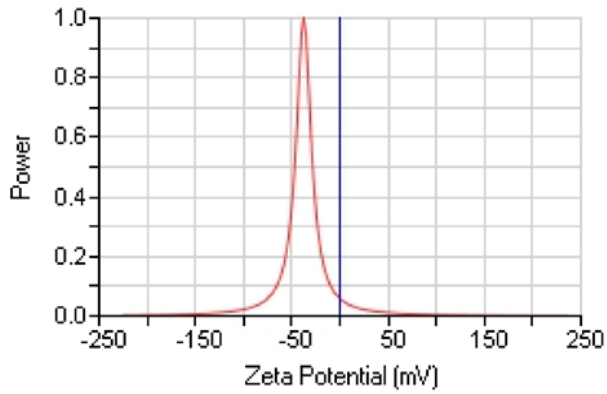

(a)

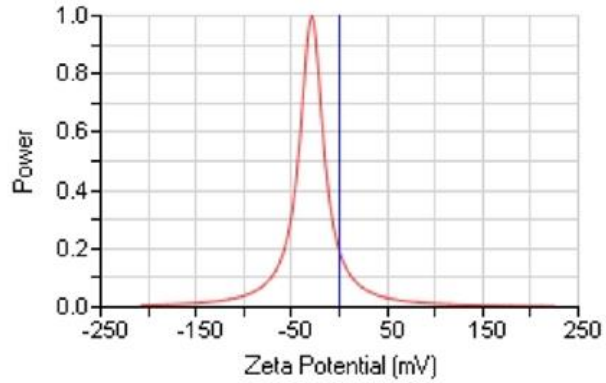

(b)

Fig. 9. Zeta potential of (CuO/ZnO) NCs: (a) calcined and (b) and not calcined

4. Photocatalytic Efficiency

The photocatalytic performance of a green-produced CuO/ZnO NCs was evaluated by studying the degradation of TC in a visible annular-type photoreactor under UV light irradiation. Exposing the specimen to light initiates the real study because the semiconducting ZnO absorbs the photon of energy from the CuO NC, which has a higher bandgap. As seen in Eqs. (1) and (2), visible light photons are expected to stimulate the valence electrons of CuO due to their small bandgap energy. This process creates a hole in the valence band (V_B) of CuO, which then moves towards ZnO, causing reduction processes and the production of superoxide ions, as in Eq. (3). Therefore, the electrons created by light can only transfer from the conduction band (C_B) of CuO to the conduction band of ZnO due to the difference in their C_B energy levels [33]. The transfer of electrons from the conduction band of ZnO to the valence band of CuO is relatively unlikely. Instead, the presence of a hole enables oxidation reactions to occur, resulting in the generation of hydroxyl radical $^{\bullet}OH$ and hydroperoxyl H_2O_2 species, as in Eq. (5). These species exhibit a high level of effectiveness in breaking down organic contaminants [36]. Radical oxidation species, such as $^{\bullet}O^{2-}$ and $^{\bullet}OH$, oxidise pollutants (TC) into degradation products, as in Eqs. (7) and (8). Thus, the heterojunction created by mixing ZnO and CuO limits the recombination of photogenerated pairs, allowing for improved oxidative species formation [25]. The inclusion of CuO reduces electron/hole recombination and enhances the formation of active radicals, resulting in a higher rate of organic pollutant degradation [31].

ZnO + hν (visible light) → ZnO (e^-_{CB} +h^+_{VB}) …(1)
CuO + hν (visible light) → CuO (e^-_{CB} +h^+_{VB}) …(2)
$O_2 + e^-$ →• O_2^- (Superoxide radicals) …(3)
• O_2^- + H_2O → HO_2• (hydroperoxy) +OH^- …(4)
HO_2 • +H_2O → H_2O_2 + •OH(hydroxyl radicals) …(5)
H_2O + h^+ → •OH + H+ …(6)
•O_2^- + organic pollutants → degraded products …(7)
•OH + organic pollutants → degraded products …(8)

The photodegradation of TC in the presence of as-prepared NPs was examined under UV-A light, and the extent of degradation was measured in terms of the absorbance of the TC solution by using a UV–Vis spectrophotometer after certain intervals of time for 180 min [37]. Figure 10 showcases the results of the degradation studies, revealing an increase in TC degradation with increasing irradiation time. Experiments were conducted to test the efficiency of different ratios of Cu to Zn (1:3, 1:6, 1:9 and 1:12). The results indicated that the ratio of 1:6 had the best degree of removal efficacy amongst all ratios when the CuO/ZnO NC dose, pH, initial concentration, temperature, agitation speed and time were set to 0.5 g.L^{-1}, 7, 10 mg.L^{-1}, 25 °C, 300 rpm and 180 min, respectively.

The degradation rate increased with increasing amounts of copper in 1:6 ratio, but when copper decreased in 1:9 and 1:12 ratios, the photocatalytic activity decreased due to the higher bandgap for ZnO NPs than for CuO/ZnO NCs. This finding indicated that an increase in CuO amount in NCs resulted in a decrease in the energy bandgap, which improves visible light harvesting and decreases photocatalytic activity. Still, in the 1:3 ratio, the photocatalytic activity decreased as the amount of copper increased. A higher percentage of copper covered the ZnO surface, reducing light absorption [33, 38]. The absorbance spectra of TC clearly showed that the TC solution was degraded by 47.8%, 72.1%, 53.08% and 53.9% after 180 min in the presence of green-synthesized CuO/ZnO NCs.

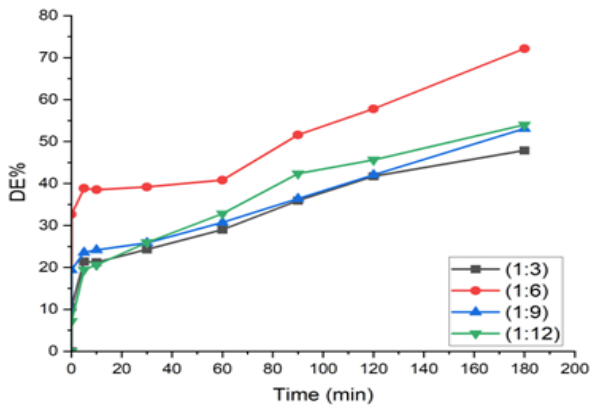

Fig. 10. TC removal for the ratios of Cu to Zn (1:3, 1:6, 1:9 and 1:12) at CuO/ZnO NC dose, pH, initial concentration, temperature, agitation speed and time of 0.5 g.L^{-1}, 7, 10 mg.L^{-1}, 25 °C, 300 rpm and 180 min, respectively.

5. Conclusion

This study presents a cost-effective and environmentally friendly solution to the water purification problem. Eucalyptus leaf extract was used for capping and reducing agents at four molar ratios of copper to zinc for the biosynthesis of CuO/ZnO NCs. These ratios were characterised using FTIR, FE-SEM, EDAX, AFM, XRD, BET and zeta potential. The calcined CuO/ZnO NCs and the sphere and a few nanorods of the non-calcined CuO/ZnO NCs demonstrated average diameters of 14 and 27 nm, respectively, and surface areas of 25.95 and 49.75 m^2/g, respectively. During the process setup, different molar ratios (1:3, 1:6, 1:9 and 1:12) of CuO/ZnO NCs were used to degrade TC through photocatalytic reactions. The results showed the 1:6 ratio was better at photocatalytic drug removal than the other molar ratios. It was able to remove 72.15% of the drug at an NC dose of 0.5 g.L^{-1}, pH 7, an initial concentration of 10 mg.L^{-1}, a temperature of 25 °C and a contact time of 180 minutes.

Acknowledgement

The authors express their profound gratitude to the Department of Biochemical Engineering at Al Khwarizmi College of Engineering, University of Baghdad, Iraq, and Nahrain University for providing facilities for the characterisation of NPs. The authors would also like to thank the Environment and Water Directorate of the Ministry of Science and Technology in Iraq for providing all the required facilities and Dr Benyamin Laboratories, Tehran University, North Karegar Ave, Tehran, Iran, for their remarkable scientific support.

References

[1] M. H. Mahdi, T. J. Mohammed, and J. A. Al-Najar, "Removal of tetracycline antibiotic from wastewater by fenton oxidation process," Eng. Technol. J, vol. 39, pp. 260–267, 2021.

[2] V. M. Mboula, V. Hequet, Y. Gru, R. Colin, and Y. Andres, "Assessment of the efficiency of photocatalysis on tetracycline biodegradation," J. Hazard. Mater., vol. 209, pp. 355–364, 2012.

[3] M. Malakootian, S. N. Asadzadeh, M. Mehdipoor, and D. Kalantar-Neyestanaki, "A new approach in photocatalytic degradation of tetracycline using biogenic zinc oxide nanoparticles and peroxymonosulfate under UVC irradiation," Desalin Water Treat, vol. 222, no. 302–312, p. 2021, 2021.

[4] M. Patel, R. Kumar, K. Kishor, T. Mlsna, C. U. Pittman Jr, and D. Mohan, "Pharmaceuticals of emerging concern in aquatic systems: chemistry, occurrence, effects, and removal methods," Chem. Rev., vol. 119, no. 6, pp. 3510–3673, 2019.

[5] A. Chen, Y. Chen, C. Ding, H. Liang, and B. Yang, "Effects of tetracycline on simultaneous biological wastewater nitrogen and phosphorus removal," RSC Adv., vol. 5, no. 73, pp. 59326–59334, 2015.

[6] S. Yang, J. Cha, and K. Carlson, "Simultaneous extraction and analysis of 11 tetracycline and sulfonamide antibiotics in influent and effluent domestic wastewater by solid-phase extraction and liquid chromatography-electrospray ionization tandem mass spectrometry," J. Chromatogr. A, vol. 1097, no. 1–2, pp. 40–53, 2005.

[7] A. Pena, M. Paulo, L. J. G. Silva, M. Seifrtová, C. M. Lino, and P. Solich, "Tetracycline antibiotics in hospital and municipal wastewaters: a pilot study in Portugal," Anal. Bioanal. Chem., vol. 396, pp. 2929–2936, 2010.

[8] P.-H. Chang et al., "Sorptive removal of tetracycline from water by palygorskite," J. Hazard. Mater., vol. 165, no. 1–3, pp. 148–155, 2009.

[9] J. E. Kim et al., "Adsorptive removal of tetracycline from aqueous solution by maple leaf-derived biochar," Bioresour. Technol., vol. 306, p. 123092, 2020.

[10] C. F. Couto, L. C. Lange, and M. C. S. Amaral, "A critical review on membrane separation processes applied to remove pharmaceutically active compounds from water and wastewater," J. Water Process Eng., vol. 26, pp. 156–175, 2018.

[11] M. Klavarioti, D. Mantzavinos, and D. Kassinos, "Removal of residual pharmaceuticals from aqueous systems by advanced oxidation processes," Environ. Int., vol. 35, no. 2, pp. 402–417, 2009.

[12] P. Liu, H. Zhang, Y. Feng, F. Yang, and J. Zhang, "Removal of trace antibiotics from wastewater: A systematic study of nanofiltration combined with ozone-based advanced oxidation processes," *Chem. Eng. J.*, vol. 240, pp. 211–220, 2014.

[13] R. D. C. Soltani, M. Mashayekhi, M. Naderi, G. Boczkaj, S. Jorfi, and M. Safari, "Sonocatalytic degradation of tetracycline antibiotic using zinc oxide nanostructures loaded on nano-cellulose from waste straw as nanosonocatalyst," *Ultrason. Sonochem.*, vol. 55, pp. 117–124, 2019.

[14] G. Y. Al-Kindi and S. T. Alnasrawy, "Tetracycline remove from synthetic wastewater by using several methods," *J. Ecol. Eng.*, vol. 23, no. 5, 2022.

[15] Z. A. Najm, A. M. Shakorfow, N. Al Mhanna, A. K. Hassan, and M. A. Atyia, "Green Fabrication and Characterization of Zinc Oxide Nanoparticles using Eucalyptus Leaves for Removing Acid Black 210 Dye from an Aqueous Medium," *Al-Khwarizmi Eng. J.*, vol. 19, no. 3, pp. 23–32, 2023.

[16] M. A. Atiya, A. K. Hassan, and F. Q. Kadhim, "Green Synthesis of Copper Nanoparticles Using Tea Leaves Extract to Remove Ciprofloxacin (CIP) from Aqueous Media," *Iraqi J. Sci.*, pp. 2832–2854, 2021.

[17] S. M. Mousavi, M. Chamack, and H. Fakhri, "Study of New Hybrid Material of ZnO/CuO and Metal-Organic Framework as Photocatalyst for Removal of Tetracycline from Water," *J. Nanostructures*, vol. 12, no. 4, pp. 1097–1107, 2022.

[18] R. A. Palominos, M. A. Mondaca, A. Giraldo, G. Peñuela, M. Pérez-Moya, and H. D. Mansilla, "Photocatalytic oxidation of the antibiotic tetracycline on TiO2 and ZnO suspensions," *Catal. Today*, vol. 144, no. 1–2, pp. 100–105, 2009.

[19] Z. X. Zhu XiangDong, W. Y. Wang YuJun, S. R. Sun RuiJuan, and Z. D. Zhou DongMei, "Photocatalytic degradation of tetracycline in aqueous solution by nanosized TiO2.," 2013.

[20] J. O. Adeyemi, D. C. Onwudiwe, and A. O. Oyedeji, "Biogenic synthesis of CuO, ZnO, and CuO–ZnO nanoparticles using leaf extracts of Dovyalis caffra and their biological properties," *Molecules*, vol. 27, no. 10, p. 3206, 2022.

[21] E. Takele, R. Feyisa Bogale, G. Shumi, and G. Kenasa, "Green synthesis, characterization, and antibacterial activity of CuO/ZnO nanocomposite using Zingiber officinale Rhizome Extract," *J. Chem.*, vol. 2023, 2023.

[22] I. Hasan, C. Shekhar, I. I. Bin Sharfan, R. A. Khan, and A. Alsalme, "Ecofriendly green synthesis of the ZnO-doped CuO@ Alg bionanocomposite for efficient oxidative degradation of p-nitrophenol," *ACS omega*, vol. 5, no. 49, pp. 32011–32022, 2020.

[23] A. B. Mapossa, W. Mhike, J. L. Adalima, and S. Tichapondwa, "Removal of organic dyes from water and wastewater using magnetic ferrite-based titanium oxide and zinc oxide nanocomposites: a review," *Catalysts*, vol. 11, no. 12, p. 1543, 2021.

[24] E. Darvishi, D. Kahrizi, and E. Arkan, "Comparison of different properties of zinc oxide nanoparticles synthesized by the green (using Juglans regia L. leaf extract) and chemical methods," *J. Mol. Liq.*, vol. 286, p. 110831, 2019.

[25] M. Hafeez *et al.*, "Eucalyptus globulus Extract-Assisted Fabrication of Copper Oxide/Zinc Oxide Nanocomposite for Photocatalytic Applications," *Crystals*, vol. 12, no. 8, p. 1153, 2022.

[26] Z. A. Najm, M. A. Atiya, and A. K. Hassan, "Biogenesis Synthesis of ZnO NPs: Its adsorption and photocatalytic activity for removal of acid black 210 dye," *Karbala Int. J. Mod. Sci.*, vol. 9, no. 3, p. 15, 2023.

[27] R. A. Basit *et al.*, "Successive photocatalytic degradation of methylene blue by ZnO, CuO and ZnO/CuO synthesized from coriandrum sativum plant extract via green synthesis technique," *Crystals*, vol. 13, no. 2, p. 281, 2023.

[28] M. T. Maru *et al.*, "Effect of Musa acuminata peel extract on synthesis of ZnO/CuO nanocomposites for photocatalytic degradation of methylene blue," *Green Chem. Lett. Rev.*, vol. 16, no. 1, p. 2232383, 2023.

[29] H. Ullah, L. Mushtaq, Z. Ullah, A. Fazal, and A. M. Khan, "Effect of vegetable waste extract on microstructure, morphology, and photocatalytic efficiency of ZnO–CuO nanocomposites," *Inorg. Nano-Metal Chem.*, vol. 51, no. 7, pp. 963–975, 2021.

[30] M. A. Atiya, A. K. Hassan, and Z. A. Mahmoud, "Fenton-like degradation of direct blue dye using green synthesised Fe/Cu bimetallic nanoparticles," *J. Environ. Eng. Sci.*, vol. 18, no. 1, pp. 43–58, 2022.

[31] K. V Chandekar *et al.*, "Visible light sensitive Cu doped ZnO: facile synthesis, characterization and high photocatalytic response," *Mater. Charact.*, vol. 165, p. 110387, 2020.

[32] A. K. Hassan, M. A. Atiya, and I. M. Luaibi, "A green synthesis of Iron/Copper nanoparticles as a catalytic of fenton-like reactions for removal of orange G Dye," *Baghdad Sci. J.*, vol. 19, no. 6, p. 1249, 2022.

[33] N. T. T. Vo, S.-J. You, M.-T. Pham, and V. Van Pham, "A green synthesis approach of pn CuO/ZnO junctions for multifunctional photocatalysis towards the degradation of contaminants," *Environ. Technol. Innov.*, vol. 32, p. 103285, 2023.

[34] I. M. Luaibi, M. A. Atiya, A. K. Hassan, and Z. A. Mahmoud, "Heterogeneous catalytic degradation of dye by Fenton-like oxidation over a continuous system based on Box–Behnken design and traditional batch experiments," *Karbala Int. J. Mod. Sci.*, vol. 8, no. 2, pp. 9–28, 2022.

[35] Z. A. Mahmoud, M. A. Atyia, and A. K. Hassan, "The Influence of Support Materials on The Photo-Fenton-like Degradation of Azo Dye Using Continuous Nanoparticles Fixed-bed Column," *Al-Khwarizmi Eng. J.*, vol. 18, no. 4, pp. 14–31, 2022.

[36] M. C. de Oliveira *et al.*, "Connecting theory with experiment to understand the photocatalytic activity of CuO–ZnO heterostructure," *Ceram. Int.*, vol. 46, no. 7, pp. 9446–9454, 2020.

[37] P. Dwivedi *et al.*, "Photoremediation of methylene blue by biosynthesized ZnO/Fe3O4 nanocomposites using Callistemon viminalis leaves aqueous extract: a comparative study," *Nanotechnol. Rev.*, vol. 10, no. 1, pp. 1912–1925, 2021.

[38] A. G. Bekru, L. T. Tufa, O. A. Zelekew, M. Goddati, J. Lee, and F. K. Sabir, "Green Synthesis of a CuO-ZnO Nanocomposite for Efficient Photodegradation of Methylene Blue and Reduction of 4-Nitrophenol," *ACS Omega*, vol. 7, no. 35, pp. 30908–30919, 2022, doi: 10.1021/acsomega.2c02687.

نهج التخليق الحيوي للمركبات النانوية CuO/ZnO باستخدام أوراق اليوكاليبتوس للتحلل الضوئي للتتراسيكلين

مروة سعد عبد الأمير[1] ، محمد عبد عطية السراج[2]* ، أحمد خضير حسان[3]، عبد المالك ميلاد شاكر[4] ، نجاح المحنا[5]

[2،1] قسم الهندسة الكيمياوية الحيوية، كلية الهندسة الخوارزمي، جامعة بغداد، بغداد، العراق

[3] مديرية البيئة والمياه والطاقة المتجددة، وزارة العلوم والتكنولوجيا، بغداد، العراق

[4] جامعة المرقيب / ليبيا

[5] الجامعة الألمانية للتكنولوجيا في عمان/عمان

* البريد الإلكتروني: atiya@kecbu.uobaghdad.edu.iq

الخلاصة

في هذه الدراسة، تم دراسة التحلل الضوئي للتتراسيكلين (TC) ، المسؤول عن تلوث المياه، في محلول مائي باستخدام نوعين من الجسيمات النانوية على أساس التخليق الأخضر لجسيمات أوكسيد الزنك النانوية (ZnO NPs) وجسيمات أوكسيد النحاس النانوية (CuO NPs) كمحفز ضوئي. تم اختيار مستخلص نبات اليوكاليبتوس كعامل اختزال وتغطية جيدة بسبب خصائصه الفعالة من حيث التكلفة وكونه مادة غير سامة وسهولة استخدامه. من ناحية أخرى، يتم تحضير نسب مولية مختلفة من النحاس: الزنك (1:3، 1:6، 1:9، 1:12)، ومن ثم يتم تقييم هذه النسب لاختيار النسبة الفعالة لإزالة الدواء (TC) أظهرت أفضل نسبة لأوكسيد النحاس/أوكسيد الزنك (1:6) أفضل أداء تحفيزي ضوئي، حيث أدت إلى تحلل 72.15% من TC عند جرعات المحفز 0.5 ZnO/CuO NCs جم، والتركيز الأولي 10 مجم/لتر، ودرجة الحموضة 7، وسرعة الخلط 300 دورة في الدقيقة، ودرجة حرارة 25 درجة مئوية، وكثافة الأشعة فوق البنفسجية 15 واط / م ^{2} والوقت 180 دقيقة. تمت دراسة خصائص الجسيمات النانوية CuO/ZnO باستخدام العديد من التقنيات التحليلية، بما في ذلك التحليل المحتمل-FT IR وFE-SEM وEDAX وAFM وBET وZeta قامت الدراسة بتحليل بنية الجسيمات النانوية، وتشكلها، والسلوك الحراري، والتركيب الكيميائي، والخصائص البصرية. أثبتت صور FE-SEM أن (1:6) CuO/ZnO NCs المكلسنة وغير المكلسنة بحجم 13.92 نانومتر و26.73 نانومتر، على التوالي، كانت بلورية وكروية. تم فحص كمية تحلل الدواء TC بواسطة NCs باستخدام التحليل الطيفي للأشعة فوق البنفسجية. هذه الطريقة مستدامة وسليمة بيئيًا لأنها تقوم بتركيب كلا الجزيئات النانوية من مصادر نباتية. يمكن استخدام هذه الجسيمات النانوية الهجينة لمعالجة المستحضرات الصيدلانية الأخرى الخطرة من أجل تقليل التلوث في المياه.